Linear Scan Voltammetry of Two-Step Irreversible Electron Oxidation Enhanced by the Immobilization of an Intermediate (E↓E) on the Electrode Surface

Milivoj Lovrić

Divkovićeva 13, Zagreb, Croatia
Corresponding author: milivojlovric13@gmail.com

Received 07/11/2022; accepted 20/02/2023
https://doi.org/10.4152/pea.2024420305

Abstract
This study performed LSV simulation of two-step irreversible electron oxidation with the intermediate (E↓E), which was immobilized on the electrode surface. The response exhibited either one or two peaks, depending on the intermediate stability. The first electron transfer depended on the reactant diffusion, while the second one was a function of the accumulated intermediate. For this reason, the second I_p was higher than the first one, and the single peak split into two peaks, under the influence of an increased SR. Thermodynamic and kinetic parameters influence on the two components of the response were analyzed.

Keywords: EE mechanism; intermediate immobilization; kinetic stabilization; two-step electron oxidation; voltammetry.

Introduction•

Responses of electrode reactions consisting of two-step electrons transfer depend on the intermediates stability [1-4]. Thermodynamically unstable intermediates can be kinetically stabilized, if the second charge transfer is slow [1, 2]. Furthermore, the intermediate can be stabilized by the complexation with metal ions [5, 6], or by the adsorption onto the electrode surface [7-11]. Particularly interesting are the reactions in which the product of the first charge transfer is a radical that is only stable if it is bound to the electrode material [12-16]. What is specific is that there are no dissolved radicals, and no adsorption equilibrium can be postulated. The intermediate appears in the form of an electroactive monolayer film, and its activity is proportional to the surface concentration. This mechanism is important for the electrochemistry of organic compounds, such as methanol [17-20] and formic acid [21-23], for Ru surface oxidation [24], and ammonia electro-oxidation [25]. Since the charge transfers in this kind of electro-oxidation are irreversible, the responses depend on the two-steps kinetics [26]. In this paper, these relationships were investigated by LSV.

Model

It was assumed that the reactant and the final product of an EE mechanism were soluble, that the intermediate was immobilized at the electrode surface, and that it

• The abbreviations and symbols definition lists are in page 230.

could not diffuse into the solution, as shown in eqs:

$$A \rightarrow R_s + e^- \quad (1)$$

$$R_s \rightarrow P + e^- \quad (2)$$

For totally irreversible electron transfers at stationary planar electrodes, the mass transfer is described by the following differential equations and starting conditions [26]:

$$\partial c_A/\partial t = D\partial^2 c_A/\partial x^2 \quad (3)$$

$$d\Gamma_R/dt = I_1/FS - I_2/FS \quad (4)$$

$$t = 0, x \geq 0: c_A = c_A^*, \Gamma_R = 0 \quad (5)$$

$$t > 0, x \rightarrow \infty: c_A \rightarrow c_A^* \quad (6)$$

$$x = 0: (\partial c_A/\partial x)_{x=0} = I_1/FS \quad (7)$$

$$I_1 = FSk_s c_{A,\,x=0} \exp[\beta_1 F (E - E^0_1)/RT] \quad (8)$$

$$I_2 = FSk_r \Gamma_R \exp[\beta_2 F (E - E^0_2)/RT] \quad (9)$$

The meanings of all symbols are in the Abbreviations list. Eqs. (3) and (4) were transformed into integral equations, and numerically solved [26]. The solution is the relationship between dimensionless current, $\Phi = (I_1 + I_2)(FSc^*)^{-1}(DvF/RT)^{-1/2}$, and E of LSV.

$$\Phi_{1,m} = \lambda_s exp(\varphi_{m,1})[1 - f\sum_{j=1}^{m-1} \Phi_{1,j} Z_{m-j+1}]/[1 + f\lambda_s exp(\varphi_{m,1})] \quad (10)$$

$$\Phi_{1,1} = \lambda_s exp(\varphi_{1,1})/[1 + f\lambda_s exp(\varphi_{1,1})] \quad (11)$$

$$t = md \quad (12)$$

$$\varphi_{m,1} = \beta_1 F(E_m - E^0_1)/RT \quad (13)$$

$$\lambda_s = k_s(DvF/RT)^{-1/2} \quad (14)$$

$$f = 2(\Delta EF/RT\pi)^{1/2} \quad (15)$$

$$\Phi_{2,m} = \lambda_r exp(\varphi_{m,2})[\sum_{j=1}^{m} \Phi_{1,j} - \sum_{j=1}^{m-1} \Phi_{2,j}]/[1 + \lambda_r exp(\varphi_{m,2})] \quad (16)$$

$$\Phi_{2,1} = \lambda_r exp(\varphi_{1,2})\, \Phi_{1,1}/[1 + \lambda_r exp(\varphi_{1,2})] \quad (17)$$

$$\varphi_{m,2} = \beta_2 F(E_m - E^0_2)/RT \quad (18)$$

$$\lambda_r = k_r \Delta E/v \quad (19)$$

In the simulation, E increment, $\Delta E = 10^{-4}$ V, was used.

Results and discussion

A typical LSV response of the EE mechanism (1) and (2), with a moderately stable intermediate, is shown in Fig. 1. The second standard E is higher than the first one, but CV exhibits a single peak at 0.280 V *vs*. E^0_1, which is close to the E_p of the second component, $E_{p,2} = 0.283$ V. The first component E_p was 0.259 V.

Kinetic parameters, λ_s and λ_r, correspond to the real rate constants, $k_s = 10^{-4}$ cm/s and $k_r = 1$ s^{-1}, which means that both electron transfers were irreversible and equally slow [25]. The response I_p, $\Phi_p = 0.89$, was close to the components sum, I_p, $\Phi_{p,1} = 0.35$ and $\Phi_{p,2} = 0.55$.

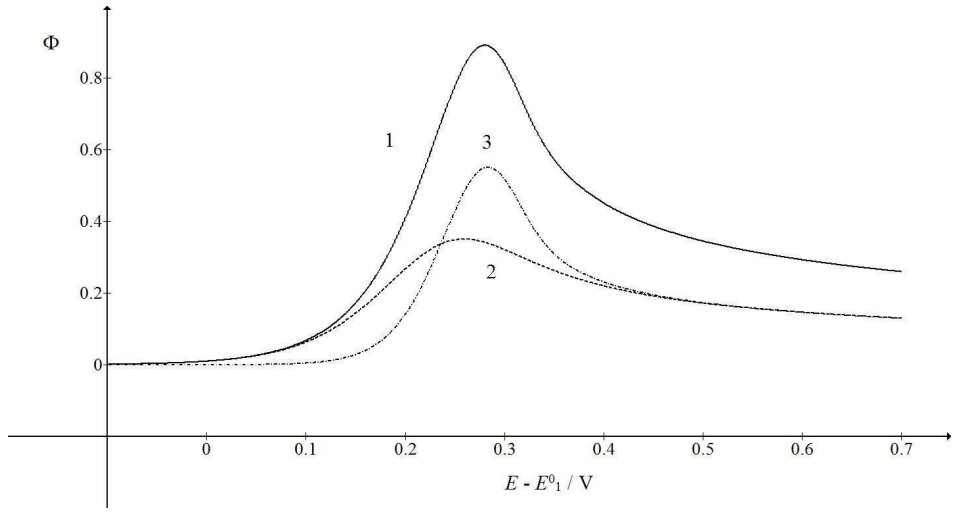

1

Figure 1: Dimensionless CV of irreversible two-step electron oxidation with: **(1)** immobilized intermediate; and its **(2)** first and **(3)** second component. $E^0_2 - E^0_1 = 0.2$ V, $\lambda_s = 10^{-2}$, $\lambda_r = 10^{-3}$, $\beta_1 = 0.5$ and $\beta_2 = 0.5$.

The first component was independent of the intermediate thermodynamic stability, but the component I_p and E_p increased with stronger second standard E. If $E^0_2 - E^0_1 < 0$ V, both components were identical, and CV was the double of the first component: $\Phi_p = 0.70$ and $E_p = 0.259$ V *vs*. E^0_1. Inversely, if $E^0_2 - E^0_1 = 0.5$ V, the response exhibited two peaks, due to the components separation, which is shown in Fig. 2.

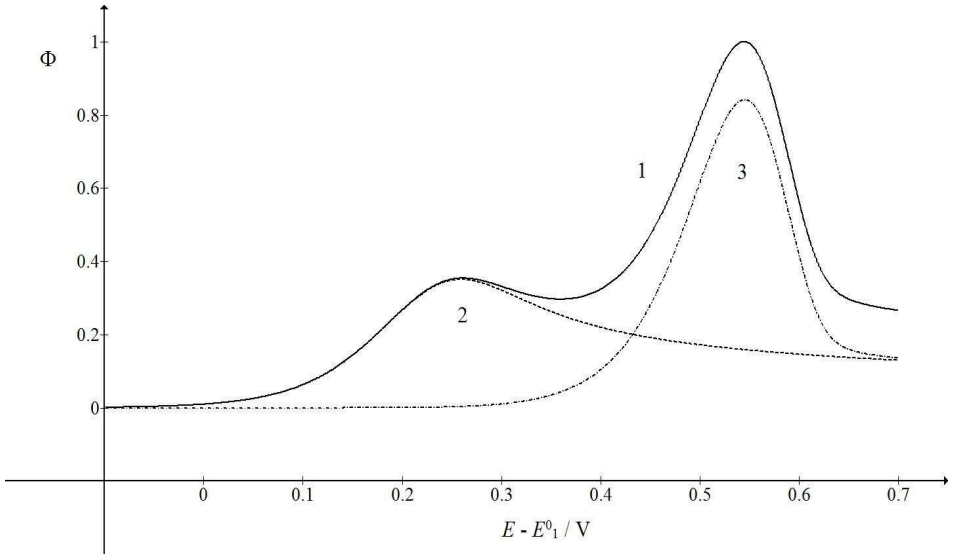

Figure 2: CV **(1)** and their components **(2, 3)**, which were calculated as $E^0_2 - E^0_1 = 0.5$ V. All other data are as in Fig. 1.

The first maximum E_p appeared at 0.259 V, and the second at 0.544 V *vs*. E^0_1. The second I_p was higher than the first one, due to the intermediate accumulation on the electrode surface. Fig. 3 shows the influence of the first kinetic parameter, λ_s, on the LSV response of the investigated EE mechanism.

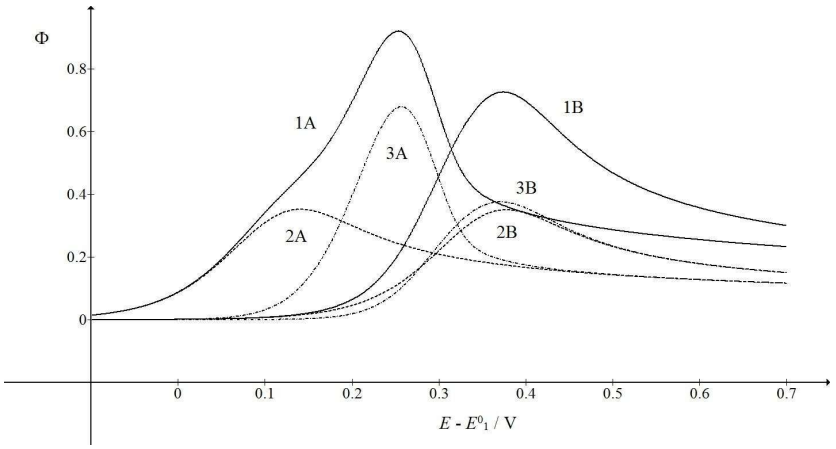

Figure 3: CV **(1)** and their components **(2, 3)**, which correspond to λ_s = **(A)** 0.1 and **(B)** 0.001. All other parameters are as in Fig. 1.

Compared to Fig. 1, the first electron transfer was either ten times faster (A) or ten times slower (B). The rate determining step of the whole mechanism was either the second electron transfer (A) or the first one (B). If the first electron transfer was relatively fast (A), the first component E_p would be $E_{p,1} = 0.141$ V, but the whole response E_p would be $E_p = 0.253$ V, which was close to the second component E_p. However, faster first steps provided intermediate higher surface concentrations, which enhanced the second component I_p. Relative slow first steps decreased the whole response. Both components E_p values were similar ($E_{p,1} = 0.377$ V and $E_{p,2} = 0.371$ V), and the first electron transfer dragged the second one towards higher E.

Fig. 4 shows the relationships between E_p and λ_s logarithm. It is seen that the first component E_p linearly depended on this argument: $E_{p,1} = E^0_1 - 0.118 \log \lambda_s + 0.023$ V.

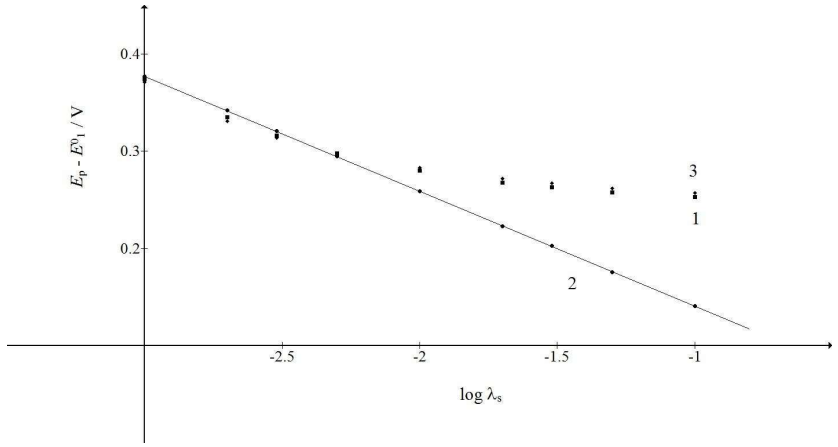

Figure 4: E_p of: **(1)** CV and its **(2)** first and **(3)** second component, as functions of the logarithm of the first electron transfer kinetic parameter. The straight line obeyed the equation: $E_{p,1} - E^0 = -118 \log \lambda_s + 0.023$ V. All other data are as in Fig.1.

If $\lambda_s \geq 10^{-2}$, E_p of the whole response would be determined by the second component E_p. If $\lambda_s \leq 5\times10^{-3}$, all E_p values would be close to the straight line in Fig. 4. These limits were applied to $\lambda_r = 10^{-3}$. Figs. 3 and 1 show the consequence of changing λ_s relative to λ_r.

The kinetic parameter variation of the second electron transfer may have caused the appearance of the two peaks maximum response, due to the intermediate stabilization. Two examples are shown in Fig. 5 (A) and (B). If $\lambda_r = \lambda_s$, both components peaks are similarly high and maximum at the same E. I_p in CV is a sum of the components I_p, because the intermediate was quickly oxidized, and its concentration at the electrode surface was low. The same response was obtained with the thermodynamically unstable intermediate. Also, if $\lambda_r = \lambda_s$ and $\lambda_s = 10^{-3}$ (see curves B in Fig. 3), I_p values would be identical to the ones in Fig. 5A, but E_p values were 118 mV higher. This is explained by equation (4), which defines the appearance and disappearance rates of the intermediate as a function of the difference between the first and the second current.

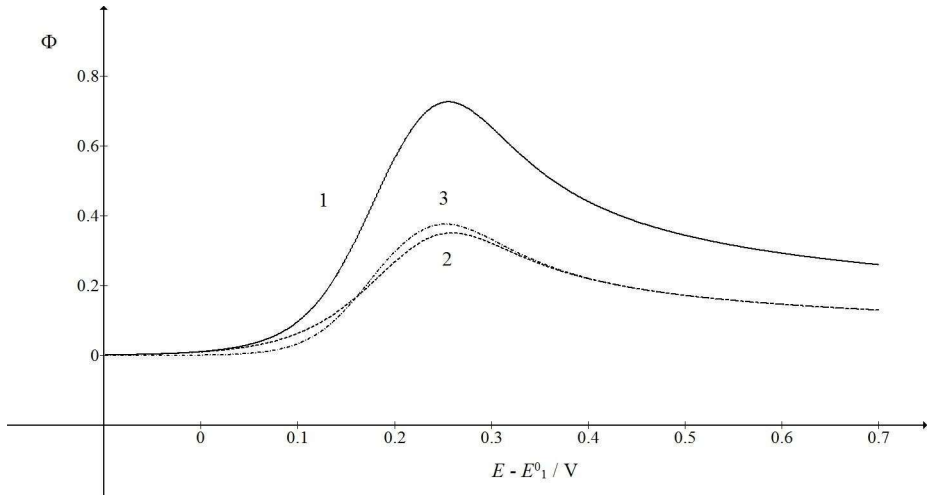

(A)

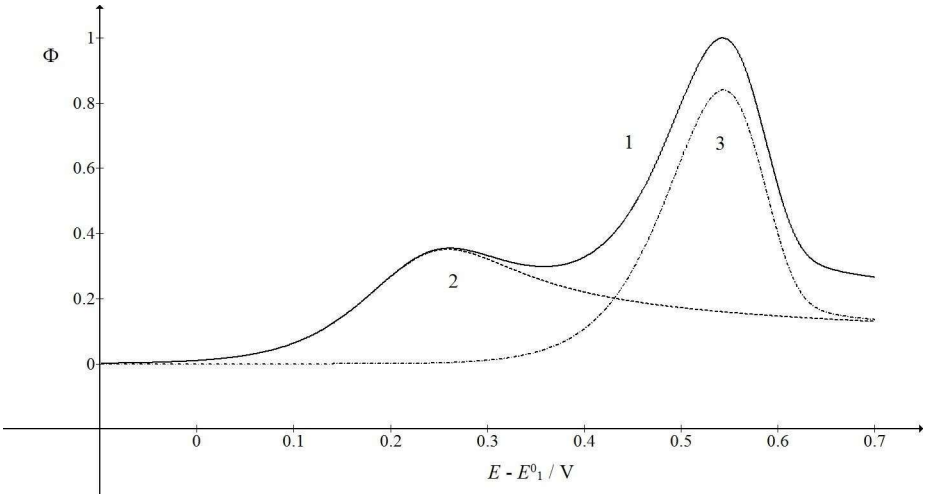

(B)

Figure 5: CV **(1)** and their components **(2, 3)**, which were calculated for $\lambda_r =$ **(A)** 10^{-2} and **(B)** 3×10^{-6}. All other data are as in Fig. 1.

The first component of the response was independent of the λ_r parameter, but the second one increased and shifted to 30 mV, if λ_r would decrease to 10^{-3}, which can be seen in Fig. 1. By λ_r further reduction, second E_p was lower, as seen in Fig. 5(B). These two peaks correspond to well separated components. The second component E_p was a linear function of the second kinetic parameter logarithm: $E_{p,2} - E^0_1 = -0.114 \log \lambda_r - 0.086$ V, which was applied to $\lambda_r < 10^{-4}$, and tended towards 0.25 V, for $\lambda_r = 10^{-2}$. The second component I_p increased with the decrease in λ_r value, due to the intermediate accumulation. The response shown in Fig. 5B is the same of the one in Fig. 2, which demonstrates that both thermodynamically and kinetically stabilized intermediates produced similar responses. Furthermore, by comparing λ_s and λ_r definitions, it is seen that their ratio depended on SR: $\lambda_s/\lambda_r = (k_s/k_r)$, $\Delta E^{-1}(\mathrm{RT/FD})^{1/2}v^{1/2}$. This means that, at higher SR, the second electron transfer was slower.

Fig. 6 illustrates the possibility that the response mode can be changed by SR variation. As λ_r depends on v, while λ_s depends on $\sqrt{v}$, change in v from 10^{-2} V/s to 1 V/s caused λ_r to diminish 100 times, but λ_s became only 10 times smaller. Considering the relationships between the first and second component, E_p and λ_s, and λ_r logarithms, respectively, it is clear why the single peak response was transformed into the two peaks response under increased SR influence. The first I_p was independent from SR, while the second one increased from 0.93 to 0.99. This means that the real currents depended not only on the reactant diffusion, but also on the intermediate accumulation on the electrode surface.

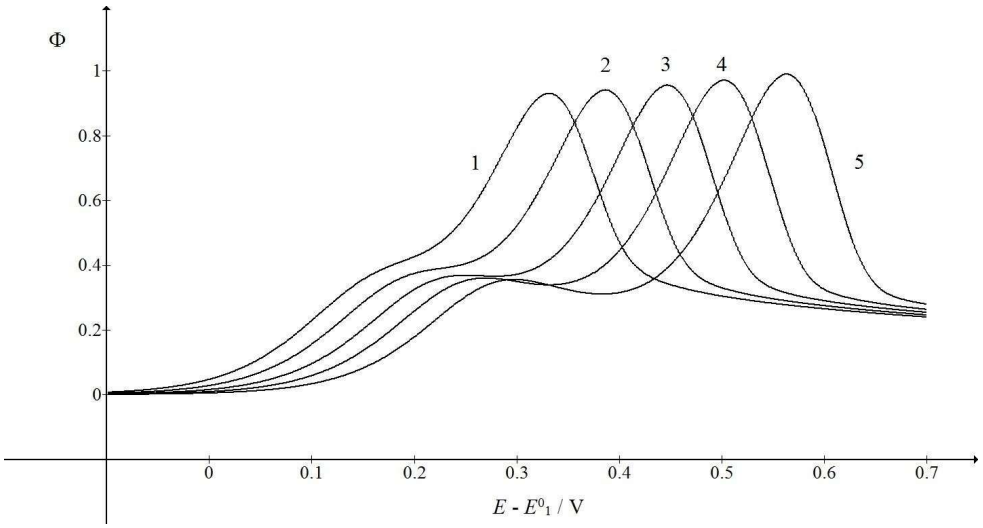

Figure 6: CV calculated for various SR. $E^0_2 - E^0_1 = 0.4$ V, $k_s = 10^{-4}$ cm/s, $k_r = 1$ s^{-1}, $D = 10^{-5}$ cm^2/s, $\Delta E = 10^{-4}$ V and v/Vs^{-1} = 0.01 (1), 0.03 (2), 0.1 (3), 0.3 (4) and 1 (5). All other data are as in Fig. 1.

Fig. 7 shows the relationships between the first and the second peak E of the split response and SR logarithm:

$$E_{p,1} - E^0_1 = 0.052 \log v + 0.297 \text{ V} \quad (20)$$

$$E_{p,2} - E^0_2 = 0.116 \log v + 0.563 \text{ V} \quad (21)$$

The straight lines slopes are close to theoretical values for totally irreversible diffusion controlled (2.3 RT/$2\beta_1 F$) and surface confined reactions (2.3 RT/$\beta_2 F$). If E^0_2 - $E^0_1 < 0.3$ V, the response exhibits a single peak at all SR, under the kinetic conditions in Fig. 6. E of this peak linearly depends on SR logarithm, with the slope that is the function of the intermediate stability. If E^0_2 - $E^0_1 = 0.2$ V, as in Fig. 1, the slope is 0.105 V, and if $E^0_2 = E^0_1$, it is 0.056 V.

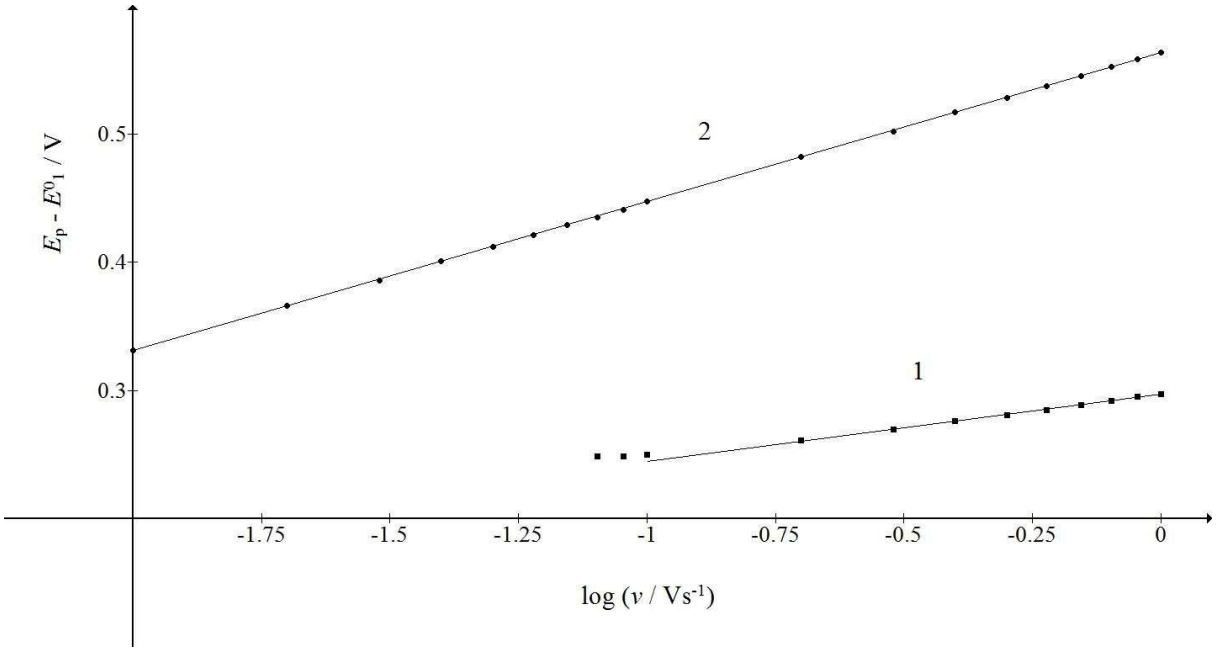

Figure 7: Dependence of the first and second maximum E_p of the split response on SR logarithm. The straight lines 1 and 2 are defined by eqs. (20) and (21). All data are as in Fig. 6.

Conclusions

LSV of the described EE mechanism may exhibit either one or two peaks, depending on the intermediate stability. The mechanism was specific, because both electron transfers were totally irreversible, and there was no adsorption equilibrium, but the intermediate was strongly and irreversibly bound to the electrode surface. Consequently, two electron transfers were mutually independent. The intermediate could be stabilized either thermodynamically or kinetically. Two standard E and two rate constants, as well as two transfer coefficients, were all independent variables. Hence, two current components were also independent of each other. Two steps of the mechanism could be recognized if the intermediate was stable, and two peaks would appear. The first peak originated from the diffusion-controlled electron transfer, and its E_p linearly depended on the SR square root logarithm. The second peak was caused by the surface confined electrode reaction, and its E_p linearly depended on SR logarithm. If the response did not split under the influence of an increased SR, the intermediate would be less stable, because either the difference between standard E was small, or the rate constants were high. The E_p of such response was also a linear function of SR logarithm, but the slope of this straight line

depended on standard E and transfer coefficients. However, EE mechanism with an immobilized intermediate could be recognized by the fact that the first I_p was smaller than the second one, due to the intermediate accumulation. In this simple model, it was assumed that no electrode surface saturation by the intermediate occurred, because it was consumed in the second electrode reaction.

Dedication

Dedicated to the memory of Dr. Šebojka Komorsky-Lovrić.

Conflict of interest

The author declares no conflict of interest.

Author's contributions

Milivoj Lovrić was the solo author.

Abbreviations

c_A^*: bulk concentration of A species (mol/cm^3)
c_A: concentration of A species (mol/cm^3)
d: time increment (s)
D: diffusion coefficient (cm^2/s)
E: potential (V)
E^0: standard potential (V)
EE: electrochemical–electrochemical
E_p: peak potential
F: Faraday constant (C/mol)
I: current (A)
I_p: peak current
k_s: standard rate constant of the first step (cm/s)
k_r: standard rate constant of the second step (s^{-1})
LSV: linear scan voltammetry
RG: constant (j/Kmol)
S: electrode surface area (cm^2)
SR: scan rate
t: time (s)
T: temperature (K)
v: scan rate (V/s)
x: distance (cm)

Meaning of symbols

β: anodic transfer coefficient
Γ_R: surface concentration of R species (mol/cm^2)

References

1. Evans DH. One-electron and two-electron transfers in electrochemistry and homogeneous solution reactions. Chem Rev. 2008;108(7):2113-2144 https://doi.org/10.1021/cr068066l

2. Galvez J, Saura R, Molina A et al. Current-potential curves with an EE mechanism. J Electroanalyt Chem. 1982;139:15-86. https://doi.org/10.1016/0022-0728(82)85101-2
3. Belding SR, Baron R, Dickinson EJF et al. Modelling diffusion effects for a stepwise two-electron reduction process at a microelectrode: study of the reduction of para-quaterphenyl in tetrahydrofuran and inference of fast comproportionation of the dianion with the neutral parent molecule. J Phys Chem C 2009;113(36):16042-16050. https://doi.org/10.1021/jp906323n
4. Molina A, Serna C, Lopez-Tenes M et al. Theoretical background for the behaviour of molecules containing multiple interacting or noninteracting redox centers in any multipotential step technique and cyclic voltammetry. J Electroanalyt Chem. 2005;576:9-19. https://doi.org/10.1016/j.jelechem.2004.09.027
5. Bogeski I, Gulaboski R, Kappl R et al. Calcium binding and transport by coenzyme Q. J Am Chem Soc. 2011;133:9293-9303. https://doi.org/10.1021/ja110190t
6. Gulaboski R, Markovska V, Jihe Z. Redox chemistry of coenzyme Q – a short overview of the voltammetric features. J Solid State Electrochem. 2016;20:3229-3238. https://doi.org/10.1007/s10008-016-3230-7
7. Kopistko OA. The galvanostatic double pulse method in the study of the kinetics of stepwise electrode processes involving the adsorption of intermediates. J Electroanalyt Chem. 1987;224:67-94. https://doi.org/10.1016/0022-0728(87)85085-4
8. Galvez J, Alcaraz ML, Park SM. Theory of the EE mechanism with adsorption of the intermediate in normal pulse polarography. J Electroanalyt Chem. 1989;266:1-9. https://doi.org/10.1016/0022- 0728(89)80210-4
9. Alcaraz ML, Galvez J. Study of the EE mechanism with adsorption of the intermediate at spherical and planar electrodes following Langmuir isotherm. Collect Czech Chem Commun. 1991;56:60-67. https://doi.org/10.1135/cccc19910060
10. Lovrić M, Komorsky-Lovrić Š. Theory of square-wave voltammetry of two-electron reduction with the adsorption of intermediate. Int J Electrochem. 2012;596268:7. https://doi.org/10.1155/2012/596268
11. Sadkowski A. Electrochemical adsorption reaction (EAR): Part I. Comparative analysis of various pulse methods in the study of equilibrium and kinetics of electrochemical adsorption reactions. J Electroanalyt Chem. 1979;105:1-23. https://doi.org/10.1016/S0022-0728(79)80335-6
12. Sadkowski A. Electrochemical adsorption reaction (EAR): Part II. Relation between large signal response and small signal (impedance) data. J Electroanalyt Chem. 1986;210:21-29. https://doi.org/10.1016/0022-0728(86)90312-8
13. Molina Concha MB, Chatenet M, Montella C et al. A faradaic impedance study of E-EAR reaction. J Electroanalyt Chem. 2013;696:24-37. https://doi.org/10.1016/j.jelechem.2013.02.013
14. Brites Helu MA, Bonazza HL, Fernandez JL. Sensing electro-adsorption reaction and surface mobility of electro-adsorbed species by scanning electrochemical induced desorption. J Electroanalyt Chem. 2016;775:64-71. https://doi.org/10.1016/j.jelechem.2016.05.031
15. Diard JP, Le Gorrec B, Montella C. Non-linear impedance for a two-step electrode reaction with an intermediate adsorbed species. Electrochim Acta. 1997;42:1053-1072. https://doi.org/10.1016/S0013- 4686(96)00206-X

16. Assiongbon KA, Roy D. Electro-oxidation of methanol on gold in alkaline media: adsorption characteristics of reaction intermediates studied using time resolved electrochemical impedance and surface plasmon resonance techniques. Surf Sci. 2005;594:99-119. https://doi.org/10.1016/j.susc.2005.07.015
17. Dobrota AS, Pašti IA. Chemisorption as the essential step in electrochemical energy conversion. J Electrochem Sci Eng. 2020;10(2):141-159. http://dx.doi.org/10.5599/jese.742
18. Mudrinić TM, Mojović ZD, Ivanović-Šašić AZ et al. Methanol electro-oxidation in alkaline solutions on platinum—based electrodes: classical and dynamical approach. Russ J Phys Chem A. 2013;87:2127-2133. https://doi.org/10.1134/S0036024413130177
19. Buck RP, Griffith LR. Voltammetric and chronopotentiometric study of the anodic oxidation of methanol, formaldehyde and formic acid. J Electrochem Soc. 1962;109(11):1005-1013.
20. Conway BE, Angerstein-Kozlowska H, Czartoryska G. "Third body" effect in the auto-inhibition of formic acid oxidation at electrodes. Electrocatalysis of formic acid and methanol oxidation at Au-Pt alloy electrodes. Z Phys Chem NF. 1978;112:195-214.
21. Freire JG, Calderon-Cardenas A, Varela H et al. Phase diagrams and dynamical evolution of the triple-pathway electro-oxidation of formic acid on platinum. Phys Chem Chem Phys. 2020;22:1078-1091. https://doi.org/10.1039/c9cp04324a
22. Lee J, Strasser P, Eiswirth M et al. On the origin of oscillations in the electrocatalytic oxidation of HCOOH on a Pt electrode modified by Bi deposition. Electrochim Acta 2001;47:501-508 https://doi.org/10.1016/S0013-4686(01)00744-7
23. Yu A, Rizo R, Vidal-Iglesias FJ et al. The surface processes on Ru/Pt(111) as probed by cyclic voltammetry and in situ surface Raman spectroscopy. ACS Sust Chem Eng. 2022;10:14824-14834. https://doi.org/10.1021/acssuschemeng.2c04584
24. Diaz LA, Botte GG. Mathematical modeling of ammonia electro-oxidation kinetics on a polycrystalline Pt rotating disk electrode. Electrochim Acta. 2015;179:510-528. https://doi.org/10.1016/j.electacta.2014.12.162
25. Lovrić M. Maxima in chronoamperometry of irreversible electrode reactions. J Electroanalyt Chem. 2021;888:115187. https://doi.org/10.1016/j.jelechem.2021.115187
26. Bieniasz LK. Modelling electrochemical experiments by the integral equation method, Springer, Berlin, 2015.